Phloretin-Induced Changes of Lipophilic Ion Transport across the Plasma Membrane of Mammalian Cells

Vladimir L. Sukhorukov,* Markus Kürschner,* Stefan Dilsky,* Thomas Lisec,† Bernd Wagner,† Wolfdieter A. Schenk,* Roland Benz,* and Ulrich Zimmermann*

*Lehrstuhl für Biotechnologie, Biozentrum, and Institut für Anorganische Chemie der Universität Würzburg, D-97074 Würzburg, Germany, and †Fraunhofer Institut Siliziumtechnologie, D-25524 Itzehoe, Germany

ABSTRACT The adsorption of the hydrophobic anion $[W(CO)_5CN]^-$ to human lymphoid Jurkat cells gave rise to an additional anti-field peak in the rotational spectra of single cells, indicating that the cell membrane displayed a strong dielectric dispersion in the kilohertz to megahertz frequency range. The surface concentration of the adsorbed anion and its translocation rate constant between the two membrane boundaries could be evaluated from the rotation spectra of cells by applying the previously proposed mobile charge model. Similar single-cell electrorotation experiments were performed to examine the effect of phloretin, a dipolar molecule known to influence the dipole potential of membranes, on the transport of $[W(CO)_5CN]^-$ across the plasma membrane of mammalian cells. The adsorption of $[W(CO)_5CN]^-$ was significantly reduced by phloretin, which is in reasonable agreement with the known phloretin-induced effects on artificial and biological membranes. The IC_{50} for the effect of phloretin on the transport parameters of the lipophilic ion was ~10 μM. The results of this study are consistent with the assumption that the binding of phloretin reduces the intrinsic dipole potential of the plasma membrane. The experimental approach developed here allows the quantification of intrinsic dipole potential changes within the plasma membrane of living cells.

INTRODUCTION

The permeability of lipophilic anions through lipid bilayer membranes is several orders of magnitude higher than that of structurally analogous cations (Andersen et al., 1976; Pickar and Benz, 1978). This observation and the results of surface potential measurements of lipid monolayers suggest that lipid bilayers possess a high intrinsic electrostatic potential termed dipole potential ψ_D. It makes the membrane interior positive by several hundreds of millivolts and is caused from the orientation of the phospholipid carbonyls and the oriented water dipoles near the surface of the membrane (McLaughlin, 1977; Pickar and Benz, 1978; Flewelling and Hubbell, 1986; Bechinger and Seelig, 1991). The dipole potential is important for a number of cellular processes associated with the plasma membrane (Antonenko et al., 1999; Cladera and O'Shea, 1998; Hertel et al., 1997; Koepsell et al., 1990).

Many studies of the dipole potential have been performed in artificial membrane systems, including planar lipid bilayers, monolayers, and liposomes, using various experimental techniques (Melnik et al., 1977; Verkman and Solomon, 1980; Reyes et al., 1983; Clarke and Kane, 1997; Cseh and Benz, 1998, 1999; Franklin and Cafiso, 1993; Pohl et al., 1997). It has been found that several dipolar compounds are able to modify the permeability properties of lipid bilayer membranes (Qin et al., 1995; Wang and Bruner, 1978). Phloretin and its structural analogs are known to enhance the cationic conductance and to decrease the anionic conductance of planar lipid bilayers containing ion carriers or hydrophobic ions (Andersen et al., 1976; Melnik et al., 1977; Reyes et al., 1983). In lipid vesicle systems, phloretin has been reported to increase both binding and translocation rates of spin-labeled hydrophobic cations and to inhibit these parameters for anionic compounds (Franklin and Cafiso, 1993). The effects of phloretin have been attributed to a reduction of the existing dipole potential ψ_D by the adsorbed phloretin molecules whose dipole moments are apparently aligned antiparallel to the intrinsic dipolar groups of the membrane (Melnik et al., 1977; De Levie et al., 1979).

The dipole potential of a lipid bilayer and its modification can be probed by studying the transport kinetics of lipophilic ions through the bilayer using the charge pulse relaxation technique (Benz and Läuger, 1977; Pickar and Benz, 1978; Cseh and Benz, 1998). Until recently, however, this experimental approach and other electrical methods were restricted to artificial bilayers or to cells and organelles of sufficiently large size for the use of intracellular electrodes.

In the present work, we applied the non-invasive single-cell electrorotation (ROT) technique (Arnold and Zimmermann, 1982) for studying the effects of phloretin on the interaction of the lipophilic anion $[W(CO)_5CN]^-$ with the plasma membrane of human lymphoblastoid cells (Jurkat line). Within a conductivity range of the external solution, the ROT spectra (i.e., the frequency dependence of the cell rotation speed) of cells treated with $[W(CO)_5CN]^-$ exhibited two well-resolved anti-field peaks, one of which was due to the capacitive charging of the plasma membrane,

Received for publication 20 November 2000 and in final form 3 May 2001.

Address reprint requests to Dr. Ulrich Zimmermann, Lehrstuhl für Biotechnologie, Biozentrum der Universität Würzburg, Am Hubland, D-97074, Würzburg, Germany. Tel.: 49-0931-888-4507; Fax: 49-0931-888-4509; E-mail: zimmermann@biozentrum.uni-wuerzburg.de.

0006-3495/01/08/1006/08 $2.00

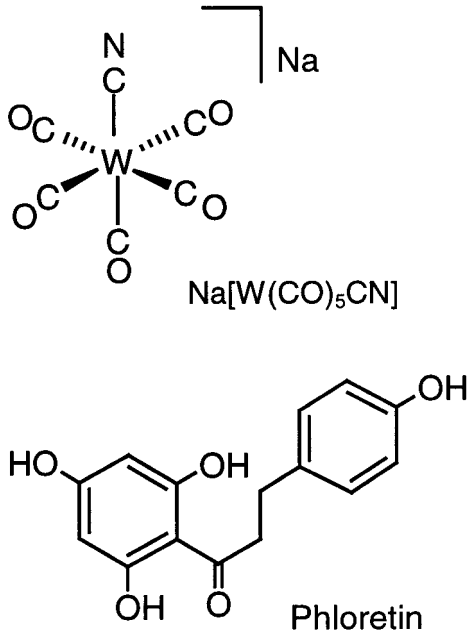

FIGURE 1 Structures of the lipophilic chemicals used here (formula, chemical name): $Na[W(CO)_5CN]\cdot 3H_2O$, sodium pentacarbonylcyanotungstate, MW of the anion 350; phloretin, 3-(4-hydroxyphenyl)-1-(2,4,6-trihydroxyphenyl)-1-propanone, MW 274.

whereas the second peak in the low-frequency range was caused by the relaxation of the lipophilic ion adsorbed to the membrane. The analysis of the ROT spectra using the previously reported model (Sukhorukov and Zimmermann, 1996) allowed the evaluation of the surface concentrations, partition coefficients, and translocation rate constants of the lipophilic ions adsorbed to the cell membrane. At micromolar concentrations, phloretin decreased markedly the adsorption of $[W(CO)_5CN]^-$, whereas the translocation rate of the anion was less sensitive to the treatment with phloretin. These data are consistent with the assumption that the adsorption of phloretin to the plasma membrane reduces the intrinsic dipole potential by 10–15 mV.

MATERIALS AND METHODS

Chemicals, buffers, and solutions

Phloretin, 3-(4-hydroxyphenyl)-1-(2,4,6-trihydroxyphenyl)-1-propanone (Fig. 1) was obtained from Fluka (Deisenhofen, Germany) and used as 10–100 mM stock solutions in ethanol. Other commercially available chemicals were from Sigma (Deisenhofen, Germany).

The tungsten carbonyl complex $Na[W(CO)_5CN]$ (Nielsen et al., 1996) was prepared by irradiating $[W(CO)_6]$ in tetrahydrofuran (THF) to produce a solution of $[W(CO)_5THF]$, and adding a stoichiometric amount of NaCN. The compound was purified by crystallization from THF/ether (with a trace of water) and characterized by elemental analyses, infrared (IR) and ^{13}C-NMR spectroscopy. The stability of its aqueous solution was checked by UV/visible and IR spectroscopy.

Cells

Human lymphoid Jurkat cells were cultured in complete RPMI 1640 growth medium containing 10% fetal calf serum (PAA, Linz, Austria) at 37°C under 5% CO_2. Every 2–3 days, the cell suspensions were diluted 1:10 with growth medium to keep the cells in the log phase. Before electrorotation, the cells were washed two to three times with and resuspended in hypo-osmolar inositol solutions (100 mOsm) at a final cell density of $(1–2) \times 10^5$ cells/ml. Phloretin and $Na[W(CO)_5CN]$ were added to the cell suspension at final concentrations of 5–250 μM and 1–50 μM, respectively. To reach partition equilibrium for the adsorption, the cells were incubated with phloretin, $Na[W(CO)_5CN]$, or both for 20–40 min before electrorotation measurements. The suspension conductivity (σ_e) was adjusted to 1–150 mS m^{-1} by addition of the appropriate amounts of HEPES-KOH, pH 7.4. For further details see Kürschner et al. (1998).

Rotation chambers and external fields

The measurements of the field frequency f_{c1} inducing fastest anti-field rotation of cells were performed under low-conductivity conditions ($\sigma_e <$ 5 mS m^{-1}) by the contra-rotating field (CRF) technique using a macroscopic four-electrode chamber that was described in detail previously (Arnold et al., 1988). Electrorotation (ROT) spectra were measured in a microstructured four-electrode chamber arranged as a planar array of circular electrodes of 60-μm diameter, 140-nm thickness (20-nm Ta and 120-nm Pt), and 200-μm electrode spacing. The microstructures were fabricated photolithographically (Fraunhofer-Institut Siliziumtechnologie, ISiT, Itzehoe, Germany). The electrodes were driven by four 90° phase-shifted, rectangular signals from a pulse generator HP 8130A (Hewlett-Packard, Boeblingen, Germany) with 2.5–4.8 V_{PP} amplitude over the frequency range from ~100 Hz to 150 MHz. A sample of cell suspension (50–70 μl) was added to the rotation chamber, and a coverslip was placed gently over its center. The cells were observed using a BX 50 Olympus microscope (Hamburg, Germany) that was equipped with a CCD video camera connected to a video monitor. ROT spectra were monitored by decreasing the field frequency in steps (five to seven frequency points per decade). At each field frequency, the rotation speed of lone cells located near the center of the chamber was determined using a stopwatch. The ROT spectra were normalized to the field strength of 1 V_{PP}/100 μm. Cell radii (a) were determined with a calibrated ocular micrometer.

Derivation of dielectric parameters of control and phloretin-treated cells

The theory of electrorotation was given in full detail in previous publications (Holzapfel et al., 1982; Arnold and Zimmermann, 1982; Fuhr and Kuzmin, 1986; Fuhr et al., 1996; Gascoyne et al., 1995; Gimsa and Wachner, 1998; Goater and Pethig, 1998; Jones, 1995). Here we will only summarize the basic assumptions and list the equations that allow the evaluation of the passive electrical cell properties from the experimental data. It is well known that the cell rotation speed Ω is determined by the imaginary part of the cell polarization, i.e., by the Clausius-Mosotti factor $U^* = (\epsilon_C^* - \epsilon_e^*)/(\epsilon_C^* + 2\epsilon_e^*)$, and is given by:

$$\Omega(f) = -\frac{\epsilon_e E^2}{2\eta} \operatorname{Im}\left(\frac{\epsilon_C^* - \epsilon_e^*}{\epsilon_C^* + 2\epsilon_e^*}\right), \qquad (1)$$

where E is the applied field strength and ϵ_e and η is the dielectric permittivity and dynamic viscosity of the external medium, respectively. The Clausius-Mosotti factor depends on the complex permittivities of the cell ϵ_C^* and the external medium ϵ_e^*. The complex permittivity of homogeneous dielectrics with conductive losses is defined as $\epsilon^* = \epsilon - j\sigma/\omega$, where ϵ and σ are the real permittivity and conductivity, respectively; $j = (-1)^{1/2}$; and $\omega = 2\pi f$ is the radian field frequency. The ROT spectra of

control and phloretin-treated cells were approximated by the simplest nondispersive single-shell model (model 1), in which a cell is viewed as a homogeneous, conducting sphere (cytosol) of radius a surrounded by a poorly conducting shell (plasma membrane) of thickness d. Taking into account that $d \ll a$, the effective complex permittivity ϵ_C^* of a cell is given by $\epsilon_C^* \approx C_m^* a \epsilon_i^*/(C_m^* a + \epsilon_i^*)$, where ϵ_i^* is the complex permittivity of the cytosol; C_m^* is the complex membrane capacitance per unit area given by $C_m^* = C_m - jG_m/\omega$, where $C_m = \epsilon_m/d$ and $G_m = \sigma_m/d$ are the specific membrane capacitance (F m^{-2}) and conductance (S m^{-2}), respectively. The ROT spectra calculated with model 1 display two Lorentzian peaks that are centered at the characteristic frequencies f_{c1} and f_{c2}. The low-frequency anti-field peak located at f_{c1} is due to the charging of the plasma membrane, whereas the high-frequency peak (f_{c2}) arises from the polarization of the cytosol.

The single-shell model also gives the following relationship between the f_{c1} peak frequency, external conductivity σ_e, cell radius a, C_m, and G_m (Arnold et al., 1988):

$$f_{c1}a = \frac{\sigma_e}{\pi C_m} + \frac{aG_m}{2\pi C_m} \quad (2)$$

This equation is based on the assumptions that 1) $\sigma_i \gg \sigma_e \gg \sigma_m$ and 2) the plasma membrane properties do not vary over the frequency range used. The mean plasma membrane parameters C_m and G_m were extracted from studying the variation of the peak frequency f_{c1} with the external conductivity σ_e (at $\sigma_e < 5$ mS m^{-1}) using the CRF technique.

Determination of the lipophilic ion binding and translocation rate constants

The treatment of mammalian cells with lipid-soluble ions can result in a strong dispersion of the electrical membrane properties in the kilohertz to megahertz range. The dispersion of C_m and G_m (i.e., their frequency dependence) arises from the relaxation of lipophilic ions adsorbed to the plasma membrane (mobile charges). In the mobile charge model (model 2) (Sukhorukov and Zimmermann, 1996), the expression for the complex membrane capacitance C_m^* is extended by the inclusion of the dispersion term $\Delta C_m/(1 + j\omega\tau_{mc})$:

$$C_m^* = C_m + \frac{\Delta C_m}{1 + j\omega\tau_{mc}} + \frac{G_m}{j\omega}, \quad (3)$$

where C_m and G_m are the high-frequency (geometrical) capacitance and the low-frequency conductance of the plasma membrane, respectively; ΔC_m and τ_{mc} are the increment and time constant of the membrane dispersion due to the adsorbed lipophilic ions. Equation 3 is based on the analysis given by Ketterer et al. (1971). The dispersion occurs at the characteristic frequency $f_{mc} = (2\pi\tau_{mc})^{-1}$, which depends on the translocation rate constant k_i of the ion across the membrane ($k_i = \pi/f_{mc}$). The increment ΔC_m is related to the surface concentration N_t mol m^{-2} of the adsorbed ions as follows: $\Delta C_m = N_t F^2/2RT$, where F, R, and T have their usual meanings. As shown elsewhere (Sukhorukov and Zimmermann, 1996; Kürschner et al., 1998, 2000), the relaxation of mobile charges gives rise to an additional anti-field peak in the low-frequency part of the ROT spectrum whose relative magnitude strongly depends on the external conductivity. In this study the ion transport parameters N_t and k_i and the electrical properties of the cytosol (ϵ_i and σ_i) were derived by fitting model 2 to the ROT spectra of individual cells treated with the lipophilic anion $[W(CO)_5CN]^-$.

RESULTS

Rotation of control and phloretin-treated cells

Rotating field frequencies giving rise to the fastest anti-field rotation (f_{c1}, see Eq. 2) of control and phloretin-treated Jurkat cells were measured under hypotonic conditions (100 mOsm) in the conductivity range from 1 to 5 mS m^{-1}. To remove the effect of variations in the cell radius a on f_{c1} (Arnold et al., 1988), the product $f_{c1}a$ is plotted versus the external conductivity in Fig. 2 *A*. A strongly linear relationship between $f_{c1}a$ and σ_e was found for all cell samples. Therefore, the membrane capacitance (C_m) and conductance (G_m) could be extracted by fitting Eq. 2 to the data from each cell sample (see Legend to Fig. 2). The mean C_m values of 7.1 ± 0.1 and 7.0 ± 0.1 mF m^{-2} were found for control cells and those treated with 250 μM phloretin,

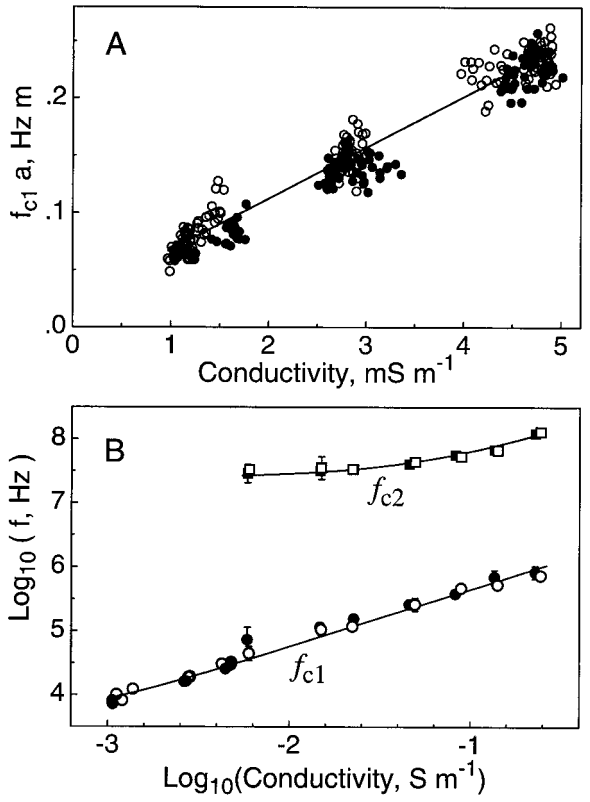

FIGURE 2 (*A*) The field frequency inducing the fastest anti-field rotation (f_{c1}) measured by the CRF technique. The cell radius (a), and the medium conductivity (σ_e) were recorded for each cell. The data for control cells (○, $N = 180$ cells) with the mean radius $\langle a \rangle = 7.6 \pm 1.0$ μm (mean ± SD), and cells treated with 250 μM phloretin (●, $N = 120$, $\langle a \rangle = 8.1 \pm 1.0$ μm) are shown. The straight line is the least-squares approximation of Eq. 2 to control data. The mean apparent membrane capacitance C_m and conductance G_m (mean ± SE) obtained from the fit are as follows: control cells, $C_m = 7.1 \pm 0.1$ mF m^{-2} and $G_m = 137 \pm 15$ S m^{-2}; phloretin-treated cells (fit not shown), $C_m = 7.0 \pm 0.1$ mF m^{-2} and $G_m = 59 \pm 43$ S m^{-2}. (*B*) Cumulative double-logarithmic plots of the characteristic anti-field (f_{c1}, ○ and ●) and co-field (f_{c2}, □ and ■) frequencies versus the external conductivity σ_e. The data were obtained by the CRF technique ($\sigma_e < 5$ mS m^{-1}) and derived from the rotational spectra ($\sigma_e > 5$ mS m^{-1}) of control cells (○ and □) and those treated with 100–250 μM phloretin (● and ■). The curves were generated with model 1 using the following parameters: $a = 7.6$ μm, $C_m = 7.1$ mF m^{-2}, $G_m = 137$ S m^{-2}, $\epsilon_i = 100\epsilon_0$, $\sigma_i = (0.35 + 3.5 \times \sigma_e)$. The assumption that σ_i depends linearly on σ_e significantly improved the fit for the f_{c2} data.

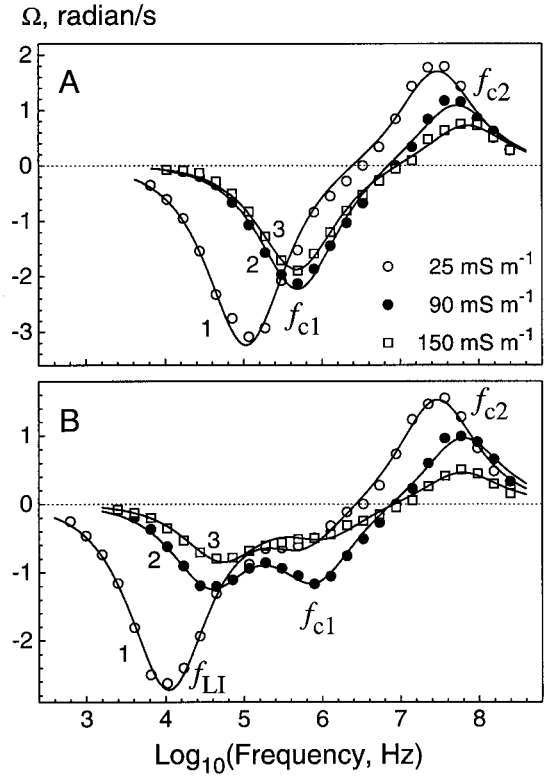

FIGURE 3 Typical rotation spectra of control Jurkat cells (*A*) and those treated with 20 μM Na[W(CO)$_5$CN] (*B*) in media of different conductivities: ~25, 90, and 150 mS m^{-1} (○, ●, and □, respectively). The rotational peaks of control cells centered at frequencies f_{c1} and f_{c2} are dominated by the plasma membrane charging and cytosol polarization, respectively. In *B*, the peak frequencies f_{LI}, f_{c1}, and f_{c2} represent the lipophilic ions, plasma membrane, and cytosolic peaks, respectively. The continuous curves show best least-squares fits of model 1 (*A*) and model 2 (*B*) to the data. In carrying out the fitting we reduced the number of unknown parameters by assuming C_m = 7.1 mF m^{-2} and G_m = 137 S m^{-2} (see Fig. 2). In *A*, fitting of model 1 to the spectra of individual cells 1, 2, and 3 (with radii a = 9, 6, and 10 μm, respectively) gave the following: σ_i = 0.41 ± 0.01, 0.52 ± 0.02, and 0.82 ± 0.05 S m^{-1} and ϵ_i/ϵ_0 = 121 ± 5, 94 ± 4, 129 ± 5 (±SE of the fits), respectively. In *B*, fitting of model 2 to the ROT spectra 1, 2, and 3 (a = 8, 8, and 10 μm) gave the following: N_t = 32 ± 2, 20 ± 1, and 17 ± 2 nmol m^{-2}; k_i = (1.6 ± 0.1, 2.2 ± 0.1, and 4.1 ± 0.4) × 10^5 s^{-1}; σ_i = 0.45, 0.82, and 0.67 S m^{-1}; and ϵ_i/ϵ_0 = 151, 132, and 126, respectively.

respectively. This means that phloretin did not cause any significant changes in the membrane capacitance.

Typical ROT spectra of control Jurkat cells measured at different external conductivities σ_e ranging from 22 to 150 mS m^{-1} are shown in Fig. 3 *A*. As expected, the anti-field plasma membrane peak (indicated by f_{c1}) moved toward higher frequency with increasing σ_e. Field frequencies above 1 MHz gave the co-field peak (f_{c2}) caused by the polarization of the cytosol. The continuous curves in Fig. 3 *A* represent the best-fit theoretical spectra to the data of control cells calculated with model 1. In carrying out the nonlinear least-squares fits, we assumed the mean membrane parameters obtained by the CRF technique (see Fig. 2 *A*). From the best fits to the ROT spectra (*curves* in Fig. 3 *A*), the cytosolic permittivity ϵ_i and conductivity σ_i for control Jurkat cells were derived (see figure legend).

The ROT spectra of Jurkat cells treated with 10–250 μM phloretin were similar if not identical to those measured on control cells at the same conductivities (data not shown). The positions of the two peaks in the ROT spectra of control and phloretin-treated cells were estimated by fitting the data by a superposition of two Lorentzian curves. The fitted f_{c1} and f_{c2} values for control and phloretin-treated cells together with the f_{c1} data obtained by the CRF technique are summarized in Fig. 2 *B*, which demonstrates that phloretin did not cause any significant changes in the passive electrical properties (i.e., C_m, G_m, σ_i, and ϵ_i) of Jurkat cells. Taken together, the linear dependence of $f_{c1}a$ on σ_e (Fig. 2 *A*), the Lorentzian shape of both ROT peaks (Fig. 3 *A*), and the good agreement of the experimental f_{c1} and f_{c2} data with the theory (Fig. 2 *B*) justify the use of model 1 for the analysis of the ROT spectra of control and phloretin-treated cells measured over the whole range of external conductivity. The internal cell structures (especially the nuclear membrane) did not show any significant influence on the ROT spectra of Jurkat cells. Note that the σ_i values decreased gradually with decreasing σ_e. This was probably caused by ion leakage out of the cytoplasm of cells, which were exposed to hypotonic low-salinity media for 20–40 min.

ROT spectra of cells treated with the lipophilic anion [W(CO)$_5$CN]$^-$

Fig. 3 *B* demonstrates drastic changes in the ROT spectra of Jurkat cells caused by [W(CO)$_5$CN]$^-$. In contrast to control and phloretin-treated cells, whose ROT spectra exhibited at a conductivity of 90 mS m^{-1} a single anti-field peak at 0.5 MHz (Fig. 3 *A*, ●), the spectra of cells treated with 20 μM [W(CO)$_5$CN]$^-$ displayed an additional, well-resolved anti-field maximum at ~40 kHz at the same conductivity (Fig. 3 *B*, ●). In these spectra, the three peaks centered at the characteristic frequencies f_{LI}, f_{c1}, and f_{c2} are dominated by the relaxation of the adsorbed lipophilic ions (mobile charges), capacitive membrane charging, and polarization of the cytosol, respectively. The conductivity-dependent changes in the ROT spectra of Jurkat cells treated with lipophilic anions (Fig. 3 *B*, spectra 1–3) were qualitatively similar to the results obtained earlier from human erythrocytes and mouse myeloma cells (Sukhorukov and Zimmermann, 1996; Kürschner et al., 1998).

The complex ROT spectra of cells treated with [W(CO)$_5$CN]$^-$ could be approximated very accurately by the mobile charge model (model 2). In Fig. 3 *B*, the fitted results are plotted as smooth curves together with the experimental ROT spectra of individual cells. For the calculation of the least-squares fits, we reduced the number of unknown parameters by using the C_m and G_m values obtained by the CRF technique (Fig. 2 *A*). From the best fits,

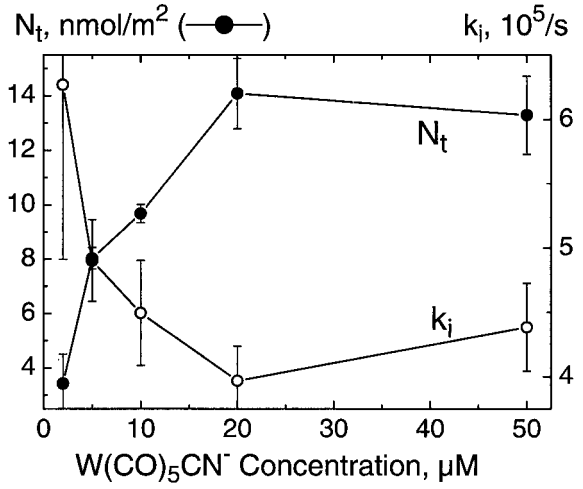

FIGURE 4 The area-specific concentration N_t (●) and translocation rate constant k_i (○) for the anion $[W(CO)_5CN]^-$ dissolved in the plasma membrane of Jurkat cells as functions of the bulk anion concentration c. The data were derived from the rotation spectra of cells measured at the conductivity of ~90 mS m^{-1}, at which the two anti-field peaks were well resolved (see curve 2 in Fig. 3 *B*). Each symbol represents the mean (±SD) from three to five individual cells.

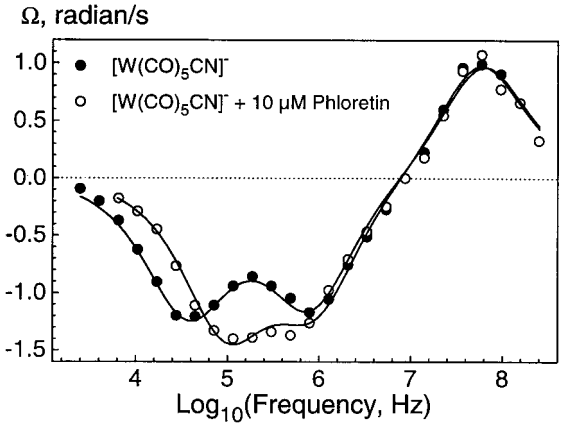

FIGURE 5 Typical rotation spectra of cells treated with 20 μM $Na[W(CO)_5CN]$ (●) and with the combination 10 μM phloretin and 20 μM $Na[W(CO)_5CN]$ (○) measured at the same conductivity (93–96 mS m^{-1}). The mobile charges' parameters extracted by fitting model 2 (*curves*) to the data shown are: 1) $N_t = 20 \pm 1$ nmol m^{-2} and $k_i = (2.2 \pm 0.1) \times 10^5$ s^{-1}; and 2) $N_t = 5.7 \pm 0.4$ nmol m^{-2} and $k_i = (4.5 \pm 0.4) \times 10^5$ s^{-1}.

the mobile charges' and cytosolic parameters, i.e., N_t, k_i, ϵ_i, and σ_i, were derived (see legend to Fig. 3 *B*).

Fig. 4 shows the N_t and k_i values evaluated from the ROT spectra of cells treated with various concentrations c of the lipophilic anion $[W(CO)_5CN]^-$. With increasing c from 2 to 20 μM, the surface concentration N_t of the anion at the membrane-water interface increased from 3.4 to its maximum value of 14 nmol m^{-2}, whereas its translocation rate constant across the membrane decreased from $\sim 6 \times 10^5$ to 4×10^5 s^{-1} ($p < 0.05$). The minimum k_i occurred at the same c of 20 μM $[W(CO)_5CN]^-$ as the maximum N_t. Further increase of c to 50 μM caused only little change in N_t and k_i. The saturation of membrane adsorption of $[W(CO)_5CN]^-$ at $c \geq 20$ μM, accompanied by a reduction of k_i, is probably caused by the generation of boundary potentials, which tend to decrease both the adsorption and transport kinetics of lipophilic ions (Benz and Läuger, 1977).

Effect of phloretin on the membrane adsorption and transport of $[W(CO)_5CN]^-$

As illustrated in Fig. 5, addition of 10 μM phloretin to cells treated with 20 μM $[W(CO)_5CN]^-$ resulted in dramatic changes in the low-frequency part of the ROT spectrum, i.e., the f_{LI} peak was shifted from 36 to 100 kHz. The observed alterations in the ROT spectrum indicate that phloretin strongly affects the interaction of $[W(CO)_5CN]^-$ with the cell membrane, because the f_{LI} peak is dominated by N_t and k_i (Sukhorukov and Zimmermann, 1996). In contrast, phloretin did not cause any significant changes in the f_{c1} and f_{c2} peak frequencies in the ROT spectra of $[W(CO)_5CN]^-$-treated cells. From the ROT spectra measured in the presence of different phloretin concentrations (5–250 μM) but at the same concentration of $[W(CO)_5CN]^-$ ($c = 20$ μM), the N_t and k_i values for the lipophilic anion dissolved in the membrane were evaluated by applying model 2 (Fig. 6). The Jurkat cells used here did not tolerate phloretin at concentrations higher than 250 μM. High micromolar concentrations of phloretin (i.e., 300 μM)

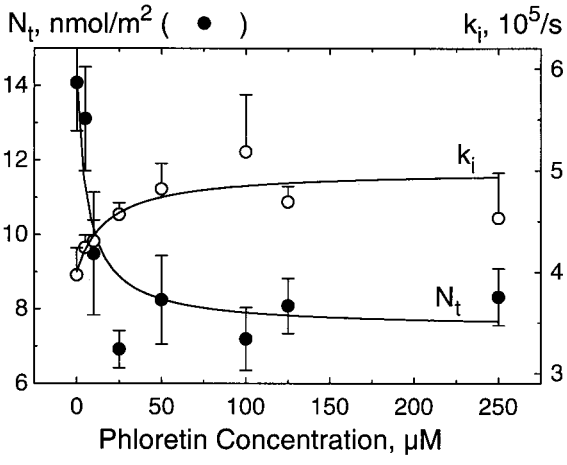

FIGURE 6 The parameters N_t (●) and k_i (○) for the anion $[W(CO)_5CN]^-$ dissolved in the plasma membrane of Jurkat cells as functions of the bulk concentration of phloretin. The data were derived from the rotation spectra measured in the presence of the same concentration of $[W(CO)_5CN]^-$ ($c = 20$ μM) in the bulk medium whose conductivity was also kept constant (~95 mS m^{-1}). Each symbol represents the mean (± SD) from three to four cells.

have also been shown to be toxic for rat pheochromocytoma cells (Hertel et al., 1997).

With increasing concentration of phloretin (Fig. 6), the membrane concentration N_t of $[W(CO)_5CN]^-$ decreased first rapidly from the initial value $N_{t0} = 14.1 \pm 1.3$ nmol m^{-2} (without phloretin) to the minimum value of 6.9 ± 0.5 nmol m^{-2} at 25 μM phloretin. Use of higher phloretin concentrations (50–250 μM) caused only little further change of the adsorption of $[W(CO)_5CN]^-$. The half-saturation constant IC_{50}, for half-maximum effect of phloretin on the $[W(CO)_5CN]^-$ binding, was found to be $IC_{50} = 10 \pm 3$ μM. The translocation rate constant k_i of the anion showed a more complicated series of relatively small changes as the phloretin concentration is increased (Fig. 6, ○).

DISCUSSION

In this study, single-cell electrorotation experiments were performed on mammalian cells treated with the lipophilic dipolar substance phloretin, with the lipophilic anion $[W(CO)_5CN]^-$, and with both agents. Neither phloretin nor $[W(CO)_5CN]^-$ nor the combination of both agents caused any significant changes in the passive electrical properties of the plasma membrane and cytoplasm (i.e., C_m, G_m, ϵ_i, and σ_i). This is in agreement with the earlier observations that treatment of mammalian cells with micromolar concentration of phloretin or $[W(CO)_5CN]^-$ does not markedly affect their plasma membrane integrity and viability (Deuticke et al., 1991; Hertel et al., 1997; Kürschner et al., 1998). We also found that phloretin produced a nearly twofold decrease in the binding of the lipophilic anion $[W(CO)_5CN]^-$ to the cell membrane, which was accompanied by a slight increase of the translocation rate of the anion across the membrane (Fig. 6).

Comparison with literature data

Phloretin readily permeates model lipid and cell membranes and also strongly binds to lipid bilayers and cytoplasmic and membrane proteins (Cseh and Benz, 1998; Krupka, 1985; Pohl et al., 1997; Reyes et al., 1983). Phloretin and its analogs have been reported to interfere with a great variety of processes associated with the cell membrane. At micromolar concentrations, this highly dipolar molecule ($\mu = 5.6$ Debye (Andersen et al., 1976) or more likely 4.6 Debye (Cseh et al., 2000)) inhibits a number of membrane transport systems, including channels and carriers for ions and nonelectrolytes (Bakker et al., 1999; Koepsell et al., 1990). Phloretin also protects human erythrocytes against electropermeabilization (Deuticke et al., 1991) and inhibits the electrostatic interaction of β-amyloid peptide with cell membranes, thus preventing the β-amyloid-induced cytotoxicity (Hertel et al., 1997).

Our finding that the adsorption of the lipophilic anion $[W(CO)_5CN]^-$ to the cell membrane could be reduced to half by phloretin (Fig. 6) agrees well with the observation that the incorporation of 5–10 mol % phloretin into phosphatidylcholine (PC) vesicles results in a two- to threefold decrease in the binding of spin-labeled hydrophobic anionic probes (Franklin and Cafiso, 1993). The ability of phloretin to inhibit the binding of lipophilic anions to membranes also accounts for the phloretin-induced reduction of the conductance of planar lipid bilayers containing lipophilic anions (Andersen et al., 1976). In lipid bilayers formed from PC, the phloretin-induced changes of the dipole potential ψ_D saturate at 30–60 μM phloretin (Pohl et al., 1997). Furthermore, as shown by the study using ψ_D-sensitive fluorescent dyes, the binding of phloretin to the plasma membrane of mouse leukemia cells saturates at 20 μM (Gross et al., 1994), which is in good agreement with the results presented in Fig. 6.

It is noteworthy that the phloretin-mediated decrease of the membrane adsorption of $[W(CO)_5CN]^-$ reported here ($IC_{50} \approx 10$ μM phloretin; see Fig. 6) occurred over the same concentration range that has previously been reported for several natural transport systems. Thus, phloretin inhibits Li^+ and Na^+ transport systems in the plasma membrane of rat hepatocytes with IC_{50} of 4 and 6 μM, respectively (Shahabi and van Rossum, 1999). Urea transport in human erythrocytes is inhibited by phloretin with IC_{50} of 25 μM (Toon and Solomon, 1987), which is closely similar to that of 21 μM found for the glucose transporter in *Trypanosoma brucei* (Bakker et al., 1999). IC_{50} for the effect on most transport systems (including that for the permeation of $[W(CO)_5CN]^-$ found in this study) coincides with the dissociation constants K_d reported for the binding of phloretin to artificial and biological membranes. Values of K_d ranging from 6 to 9 μM have been determined for the phloretin interaction with various model membranes using different experimental approaches (Verkman, 1980; Reyes et al., 1983; Awiszus and Stark, 1988; Clarke and Kane, 1997; Cseh and Benz, 1998). In erythrocytes ghosts, phloretin is found to bind with a high affinity ($K_d = 1.5$ μM) to membrane proteins and with lower affinity ($K_d = 54$ μM) to lipids (Jennings and Solomon, 1976). Despite its high affinity, phloretin is usually considered as a nonspecific transport inhibitor, whose effects are generally attributed to a reduction of the intrinsic dipole potential (ψ_D) of the lipid bilayer by the adsorbed phloretin molecules.

Estimation of the phloretin-induced changes in the membrane dipole potential

The transport parameters of the lipophilic anion presented in Fig. 6 can be used for the estimation of the phloretin-induced changes in the dipole potential $\Delta\psi_D$ of the plasma membrane. As shown by Cseh and Benz (1999), the fol-

lowing relation between $\Delta\psi_D$ and the transport kinetics of lipophilic ions holds:

$$\Delta\psi_D = -\frac{RT}{F}\ln\frac{k_{i0}\beta_0}{k_i\beta}, \quad (4)$$

where k_i and k_{i0} are the translocation rate constants of the anion $[W(CO)_5CN]^-$ in the presence and absence of phloretin, respectively, with the corresponding partition coefficients $\beta_0 = N_{t0}/2c$ and $\beta = N_t/2c$. The anion concentration in the medium c was kept constant ($c = 20\ \mu M$).

The maximum reduction of ψ_D in the cell membrane, $\Delta\psi_D$, of $-(10–15)$ mV, was found for phloretin concentrations equal to or higher than 25 μM. Using Eq. 4 and the data shown in Fig. 6, the $\Delta\psi_D$ values ($\pm$SD) of -15 ± 4, -11 ± 2, and -11 ± 3 mV were calculated for phloretin concentrations of 25, 100, and 250 μM, respectively. It has to be noted that these $\Delta\psi_D$ estimates are about one order of magnitude smaller than those reported for planar bilayers and vesicles formed from phospholipids, where the dipole potential is altered by over 120–160 mV in the presence of 300 μM and 15 mol % phloretin, respectively (Cseh and Benz, 1999; Franklin and Cafiso, 1993). In PC monolayers, the phloretin-induced ψ_D change is approximately twice as high as that measured in PC bilayers (Cseh and Benz, 1998). This means probably also that the Langmuir adsorption isotherm provides a satisfactory description of phloretin adsorption to the cell membranes because the contribution of the dipole-dipole interaction between phloretin and the membrane is rather small because of the small dipole potential change (Cseh and Benz, 1998). The reasons for the large differences between cell and model membranes remain to be elucidated. The difference between lipid bilayers and biological membranes may be caused by the presence of adsorbed and intrinsic proteins that may considerably lower the surface concentration of lipids and the membrane dipole potential. The relatively small magnitude of phloretin-induced changes of $\Delta\psi_D$ can also be explained by the method used here, which provides a $\Delta\psi_D$ value averaged over the whole cell surface. Because of the high heterogeneity of the cell membrane, however, areas might exist where strong adsorption of phloretin and, therefore, greater changes in ψ_D occur. These local alterations of ψ_D can affect significantly the kinetics of particular membrane proteins, even though the averaged dipole potential hardly changes.

The absolute value for the dipole potential in the cell membrane can also be estimated using the experimental approach described here. This can be made by comparing the membrane binding and translocation parameters of hydrophobic anions and cations with similar molecular size and shape (Pickar and Benz, 1978). Unfortunately, none of the lipophilic cations available and tested so far, including tetraphenylphosphonium (TPP^+), tetraphenylarsonium ($TPAs^+$), and $Re(CO)_6^+$, were able to introduce mobile charges into the cell membrane detectable by electrorotation. The lack of mobile charges means that lipophilic cations either do not appreciably adsorb to the cell membrane and/or they do not translocate through the membrane fast enough for determination by the ROT technique. Nontoxic lipophilic anions and cations designed to examine the intrinsic potential profile in the plasma membrane of living cells will be the subject of future research in our laboratories.

CONCLUSIONS

In this study the electrorotation technique has proved to be able to yield quantitative data on the partition and translocation kinetics of lipophilic anions in the plasma membrane of mammalian cells. Phloretin was shown to inhibit the adsorption of lipophilic anions, which can be accounted for by a lowering of the intrinsic dipole potential of the membrane. These results offer valuable insights into the relationships between the dipole potential and electrical membrane properties and also into the mechanisms of various processes, such as unassisted and carrier-mediated ion transport, charge transfer and stabilization inside biological membranes, drug delivery, etc. Furthermore, the experimental approach described here can be useful for studying the complex electrostatic phenomena occurring at the cell membrane interfaces, including ligand-receptor interactions, binding and translocation of hormones, peptides, and proteins, and also for the characterization of the chemical agents that modify the boundary potentials in cell and artificial membranes.

This work was supported by grants from the Deutsche Forschungsgemeinschaft to W.A.S. and V.L.S. (SCHE 209/17–3) and to U.Z. (Zi 99/12–1).

REFERENCES

Andersen, O. S., A. Finkelstein, I. Katz, and A. Cass. 1976. Effect of phloretin on the permeability of thin lipid membranes. *J. Gen. Physiol.* 67:749–771.

Antonenko, Y. N., T. I. Rokitskaya, and E. A. Kotova. 1999. Effect of dipole modifiers on the kinetics of sensitized photoinactivation of gramicidin channels in bilayer lipid membranes. *Membr. Cell Biol.* 13: 111–120.

Arnold, W. M., and U. Zimmermann. 1982. Rotating-field-induced rotation and measurement of the membrane capacitance of single mesophyll cells of *Avena sativa. Z. Naturforsch.* 37c:908–915.

Arnold, W. M., U. Zimmermann, W. Heiden, and J. Ahlers. 1988. The influence of tetraphenylborates (hydrophobic anions) on yeast cell electro-rotation. *Biochim. Biophys. Acta.* 942:96–106.

Awiszus, R., and G. Stark. 1988. A laser-T-jump study of the adsorption of dipolar molecules to planar lipid membranes. II. Phloretin and phloretin analogues. *Eur. Biophys. J.* 15:321–328.

Bakker, B. M., M. C. Walsh, B. H. ter Kuile, F. I. Mensonides, P. A. Michels, F. R. Opperdoes, and H. V. Westerhoff. 1999. Contribution of glucose transport to the control of the glycolytic flux in *Trypanosoma brucei. Proc. Natl. Acad. Sci. U.S.A.* 96:10098–10103.

Bechinger, B., and J. Seelig. 1991. Interaction of electric dipoles with phospholipid head groups: a ^2H and ^{31}P NMR study of phloretin and

phloretin analogues in phosphatidylcholine membranes. *Biochemistry.* 30:3923–3929.

Benz, R., and P. Läuger. 1977. Transport kinetics of dipicrylamine through lipid bilayer membranes: effects of membrane structure. *Biochim. Biophys. Acta.* 468:245–258.

Cladera, J., and P. O'Shea. 1998. Intramembrane molecular dipoles affect the membrane insertion and folding of a model amphiphilic peptide. *Biophys. J.* 74:2434–2442.

Clarke, R. J., and D. J. Kane. 1997. Optical detection of membrane dipole potential: avoidance of fluidity and dye-induced effects. *Biochim. Biophys. Acta.* 1323:223–239.

Cseh, R., and R. Benz. 1998. The adsorption of phloretin to lipid monolayers and bilayers cannot be explained by Langmuir adsorption isotherms alone. *Biophys. J.* 74:1399–1408.

Cseh, R., and R. Benz. 1999. Interaction of phloretin with lipid monolayers: relationship between structural changes and dipole potential change. *Biophys. J.* 77:1477–1488.

Cseh, R., M. Hetzer, K. Wolf, J. Kraus, G. Bringmann, and R. Benz. 2000. Interaction of phloretin with membranes: on the mode of action of phloretin at the water-lipid interface. *Eur. Biophys. J.* 29:172–183.

De Levie, R., S. K. Rangarajan, P. F. Seelig, and O. S. Andersen. 1979. On the adsorption of phloretin onto a black lipid membrane. *Biophys. J.* 25:295–300.

Deuticke, B., Lütkemeier, P., and B. Pose. 1991. Influence of phloretin and alcohols on barrier defects in the erythrocyte membrane caused by oxidative injury and electroporation. *Biochim. Biophys. Acta.* 1067: 111–122.

Flewelling, R. F., and W. L. Hubbell. 1986. The membrane dipole potential in a total membrane potential model: applications to hydrophobic ion interactions with membranes. *Biophys. J.* 49:541–552.

Franklin, J. C., and D. S. Cafiso. 1993. Internal electrostatic potentials in bilayers: measuring and controlling dipole potentials in lipid vesicles. *Biophys. J.* 65:289–299.

Fuhr, G., and P. I. Kuzmin. 1986. Behavior of cells in rotating electric fields with account to surface charges and cell structures. *Biophys. J.* 50:789–795.

Fuhr, G., U. Zimmermann, and S. G. Shirley. 1996. Cell motion in time-varying fields: principles and potential. *In* Electromanipulation of Cells. U. Zimmermann and G. Neil, editors. CRC Press, Boca Raton, FL. 259–328.

Gascoyne, P. R. C., F. F. Becker, and X.-B. Wang. 1995. Numerical analysis of the influence of experimental conditions on the accuracy of dielectric parameters derived from electrorotation measurements. *Bioelectrochem. Bioenerg.* 36:115–125.

Gimsa, J., and D. Wachner. 1998. A unified resistor-capacitor model for impedance, dielectrophoresis, electrorotation, and induced transmembrane potential. *Biophys. J.* 75:1107–1116.

Goater, A. D., and R. Pethig. 1998. Electrorotation and dielectrophoresis. *Parasitology.* 117:S177–S189.

Gross, E., R. S. Bedlack, Jr., and L. M. Loew. 1994. Dual-wavelength ratiometric fluorescence measurement of the membrane dipole potential. *Biophys. J.* 67:208–216.

Hertel, C., E. Terzi, N. Hauser, R. Jakob-Rotne, J. Seelig, and J. A. Kemp. 1997. Inhibition of the electrostatic interaction between beta-amyloid peptide and membranes prevents beta-amyloid-induced toxicity. *Proc. Natl. Acad. Sci. U.S.A.* 94:9412–9416.

Holzapfel, C., J. Vienken, and U. Zimmermann. 1982. Rotation of cells in an alternating electric field: theory and experimental proof. *J. Membr. Biol.* 67:13–26.

Jennings, M. L., and A. K. Solomon. 1976. Interaction between phloretin and the red blood cell membrane. *J. Gen. Physiol.* 67:381–197.

Jones, T. B. 1995. Electromechanics of Particles. Cambridge University Press, New York.

Ketterer, B., B. Neumcke, and P. Läuger. 1971. Transport mechanism of hydrophobic ions through lipid bilayer membranes. *J. Membr. Biol.* 5:225–245.

Koepsell, H., G. Fritzsch, K. Korn, and A. Madrala. 1990. Two substrate sites in the renal Na^+-D-glucose cotransporter studied by model analysis of phlorizin binding and D-glucose transport measurements. *J. Membr. Biol.* 114:113–132.

Krupka, R. M. 1985. Asymmetrical binding of phloretin to the glucose transport system of human erythrocytes. *J. Membr. Biol.* 83:71–80.

Kürschner, M., K. Nielsen, C. Andersen, V. L. Sukhorukov, W. A. Schenk, R. Benz, and U. Zimmermann. 1998. Interaction of lipophilic ions with the plasma membrane of mammalian cells studied by electrorotation. *Biophys. J.* 74:3031–3043.

Kürschner, M., K. Nielsen, J. R. G. von Langen, W. A. Schenk, U. Zimmermann, and V. L. Sukhorukov. 2000. Effect of fluorine substitution on the interaction of lipophilic ions with the plasma membrane of mammalian cells. *Biophys. J.* 79:1490–1497.

McLaughlin, S. 1977. Electrostatic potentials at membrane-solution interfaces. *Curr. Top. Membr. Transp.* 9:71–144.

Melnik, E., R. Latorre, J. E. Hall, and D. C. Tosteson. 1977. Phloretin-induced changes in ion transport across lipid bilayer membranes. *J. Gen. Physiol.* 69:243–247.

Nielsen, K., W. A. Schenk, M. Kriegmeier, V. L. Sukhorukov, and U. Zimmermann. 1996. Absorption of tungsten carbonyl anions into the lipid bilayer membrane of mouse myeloma cells. *Inorg. Chem.* 35: 5762–5763.

Pickar, A. D., and R. Benz. 1978. Transport of oppositely charged lipophilic probe ions in lipid bilayer membranes having various structures. *J. Membr. Biol.* 44:353–376.

Pohl, P., T. I. Rokitskaya, E. E. Pohl, and S. M. Saparov. 1997. Permeation of phloretin across bilayer lipid membranes monitored by dipole potential and microelectrode measurements. *Biochim. Biophys. Acta.* 1323: 163–172.

Qin, Z., G. Szabo, and D. S. Cafiso. 1995. Anesthetics reduce the magnitude of the membrane dipole potential: measurements in lipid vesicles using voltage-sensitive spin probes. *Biochemistry.* 34:5536–5543.

Reyes, J., F. Greco, R. Motais, and R. Latorre. 1983. Phloretin and phloretin analogs: mode of action in planar lipid bilayers and monolayers. *J. Membr. Biol.* 72:93–103.

Shahabi, V., and G. D. V. van Rossum. 1999. Transport pathways for therapeutic concentrations of lithium in rat liver. *J. Membr. Biol.* 172: 101–111.

Sukhorukov, V. L., and U. Zimmermann. 1996. Electrorotation of erythrocytes treated with dipicrylamine: mobile charges within the membrane show their "signature" in rotational spectra. *J. Membr. Biol.* 153: 161–169.

Toon, M. R., and A. K. Solomon. 1987. Modulation of water and urea transport in human red cells: effects of pH and phloretin. *J. Membr. Biol.* 99:157–164.

Verkman, A. S. 1980. The quenching of an intramembrane fluorescent probe: a method to study the binding and permeation of phloretin through bilayers. *Biochim. Biophys. Acta.* 599:370–379.

Verkman, A. S., and A. K. Solomon. 1980. Kinetics of phloretin binding to phosphatidylcholine vesicle membranes. *J. Gen. Physiol.* 75:673–692.

Wang, C.-C., and L. J. Bruner. 1978. Lipid-dependent and phloretin-induced modifications of dipicrylamine adsorption by bilayer membranes. *Nature.* 272:268–270.